Electronic supplementary materials *Mendeleev Commun.*, 2023, **33**, 349–352

Titanium dioxide nanoparticles heavily doped with niobium: a light-induced electron paramagnetic resonance study

Vladimir Yu. Osipov, Dong Hao, Kazuyuki Takai, Tetsuo Uchikoshi, Hironori Ogata and Takamasa Ishigaki

Contents

S1. Synthesis of Nb-doped TiO_2 polymorphs

All chemicals used in this study were purchased from Wako Pure Chemical Industry Ltd., Osaka, Japan, and were used as received without any purification. 25.0 at.% niobium doped TiO_2 was synthesized through radio frequency thermal plasma processing. Details of the experimental setup and synthesis process can be found elsewhere[S1,S2]. During subsequent (after synthesis) processing at a temperature of 850 °C, part of anatase is transformed into rutile, which is a gradual process. The purpose of increasing the content of rutile phase in the two-phase rutile-anatase system by the high-temperature heat-treatment was to increase the proportion of the material that can absorb visible light and work as an optical antenna. Titanium and niobium concentrations were analyzed by inductively coupled plasma atomic emission spectroscopy (ICP-AES spectrometer, model SPS-7800, Seiko Instruments Inc., Chiba, Japan).

The photocatalytic reactivity of Nb-doped TiO_2 nanopowders was quantified in terms of the degradation rates of methyl orange ($C_{14}H_{14}N_3NaO_3S$, reagent grade; Wako Pure Chemical Industries Ltd, Osaka, Japan) in aqueous TiO_2 suspension under UV (mainly 316 and 365 nm) and visible-light irradiation (mainly 405 and 436 nm) at room temperature according to the previously described method.[S2,S3] The TP-NTO850 showed the highest visible-light photocatalytic properties.[S4] Details of these studies are being finalized and will be published soon.

S2. Characterization

Electron paramagnetic resonance

The EPR spectra of the samples were studied at Hosei University (Tokyo, Japan). They were recorded at the temperature range 100-210 K using an X-band EPR spectrometer (JEOL JES-FA 300, Japan) at a microwave frequency of ~9.078 GHz. The EPR spectrometer was equipped with an Oxford Instruments ESR 900 helium flow cryostat and an optical window for irradiating the sample with external light. The liquid nitrogen flow was used as a coolant. The accuracy of temperature stabilization was ±0.03 K. The EPR spectra were obtained after a single illumination of the sample with the light of a gas-discharge xenon lamp at a temperature of 100 K for some time. Before measuring, the selected sample was heated at 150 °C for 1 h to remove the adsorbed water. A mass of 20-25 mg of dried powder was introduced into a quartz EPR tube with an outer diameter of 5 mm. The open end of the tube was sealed against moisture. EPR spectra of signals with *g*-factors $g \approx 2$ were recorded in the interval from 313 to 343 mT, with microwave power of P_{MW} = 2 mW, magnetic field modulation amplitude A_m = 0.07 mT and frequency ν = 100 kHz,

amplifier gain G = 500 (or less), and N=8 (or 10) signal accumulation cycles. The time constant was 0.03 s, and the total recording time for the magnetic field sweep over the 314 to 343 mT interval was 60 s. Due to the fact that a low-temperature cryostat was used to ensure low-temperature measurements at T=100 K and there was no space between the electromagnet poles for attaching additional sensors, the refinement and correction of the magnetic field values using NMR magnetometer was not produced. The magnetic field was measured with a standard Hall sensor glued to one of the poles of an electromagnet. Note that in all presented EPR spectra the horizontal axis shows the uncorrected value of the magnetic field obtained from the Hall sensor, and for precision calculations, the magnetic field was calibrated by a Mn^{2+}/MgO marker as an external standard reference.

Illumination was carried out through an optical absorbing filter (HA30, Hoya Corporation, Japan) that excluded heating of the sample by infrared rays. The emission spectrum of the lamp and the transmission spectrum of the glass filter used are shown in Figure S1. The EPR spectra were recorded under dark conditions after the illumination source was switched off. It was also specifically verified that in the microwave power range from 0 to 8 mW, the integrated intensity of the recorded EPR signal (at 100 K, integration range 317-340 mT) follows a linear dependence on the square root of the microwave power with acceptable accuracy, and the signals taken at a power of 2 mW at various temperatures are not distorted by saturation effects.

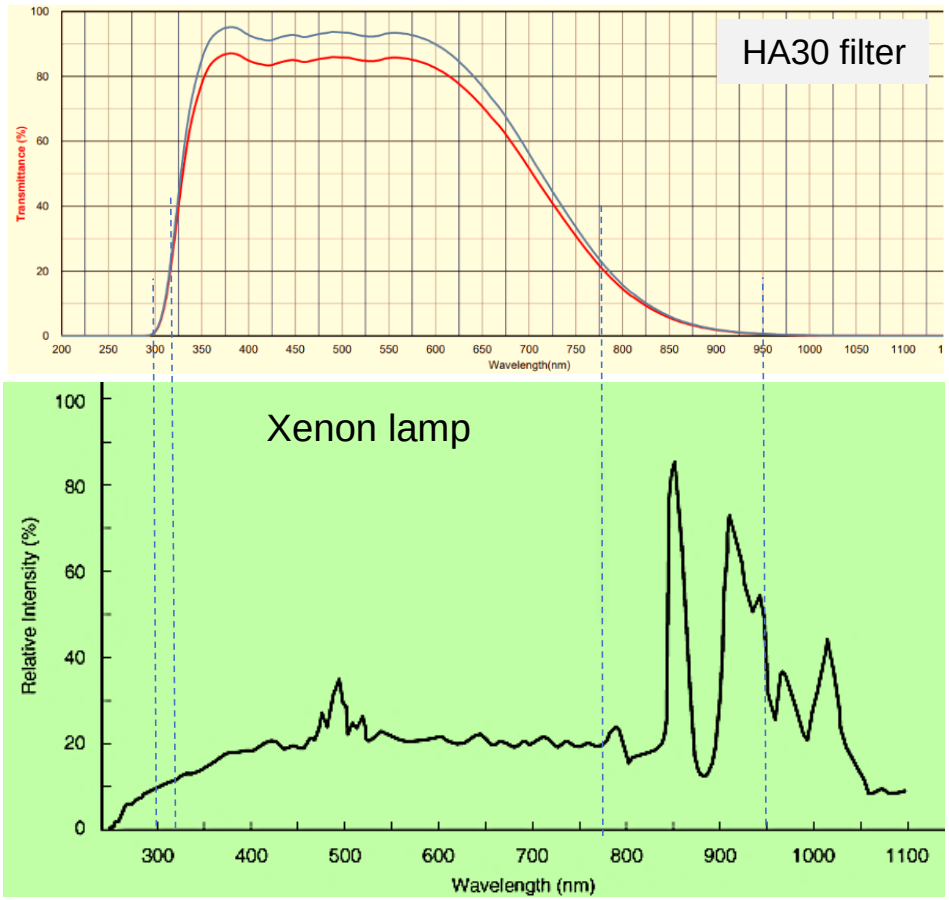

Figure S1. The emission spectrum of a xenon lamp (down) and the transmission spectrum of an HA30 optical filter (up) used to irradiate the sample with interband light at a temperature of 100 K. Upper part: total transmittance – red line, internal transmittance – blue line. The heating radiation from the lamp (in the spectral range above 900 nm) is effectively cut off by the filter.

EPR spectra taken at 100-200 K showed the presence of paramagnetic S=1/2 Ti^{3+} species in the 3+ charge state in the anatase lattice. Well-identified signatures from the EPR signals of Ti^{3+} are contained in the all spectra of sample TP-NTO850. We have studied the temperature dependence of the integral intensity of the EPR signal of the TP-NTO850 sample. With increasing temperature, this intensity decreases, but not according to the Curie law, as for ordinary paramagnetic centers with a temperature-independent concentration, but faster. To obtain points for drawing such a dependence for each recorded EPR spectrum in the form of the first derivative of absorption (with respect to the magnetic field) on the magnetic field, the integral spectrum was reconstructed. The integrated EPR spectrum from Ti^{3+} sites was obtained by numerical integration of the spectrum of the first derivative of microwave absorption with respect to the magnetic field. The corresponding intensity of the integral signal is determined by the area under the spectrum of the integral signal. Figure S2 shows as an example the spectrum of the integrated microwave absorption signal of a sample at a temperature of 150 K.

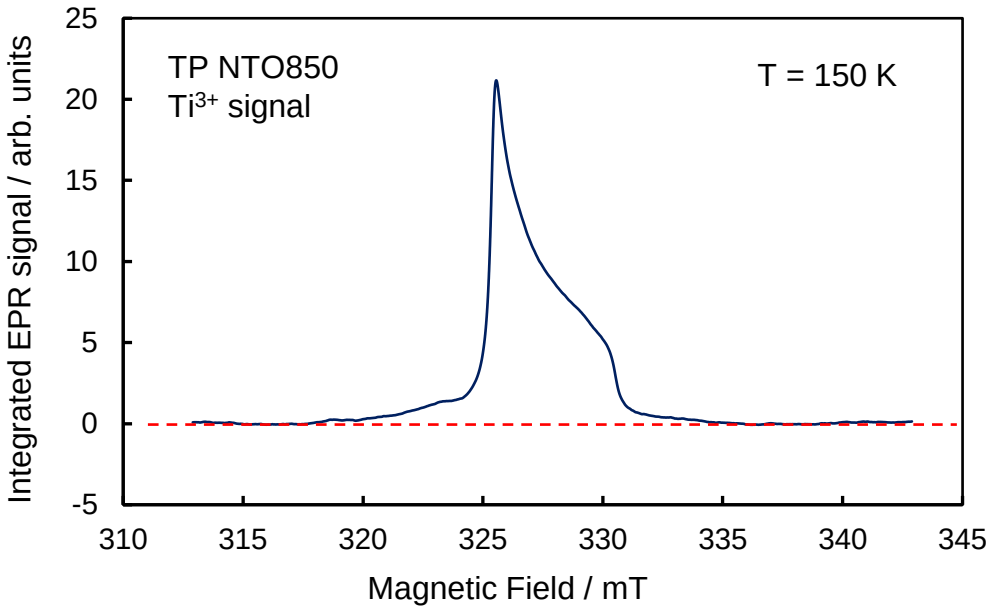

Figure S2. Integrated EPR signal from Ti^{3+} sites in the anatase phase that captured photogenerated electrons at a temperature of 150 K. The red dashed line shows the zero level of microwave absorption. Microwave frequency 9.078 GHz, microwave power 2 mW.

S3. Formation of Ti^{3+} sites upon illumination with interband light

Energy band diagrams of contacting particles of rutile and anatase and schemes of optical transitions in particles are shown in Figure S3. Upon excitation by UV-visible light, photocarriers (electrons and holes) are generated in both particles, and some of these photoelectrons are captured in the anatase particle (in the bulk or at the interface), forming long-lived paramagnetic Ti^{3+} sites at low temperatures. In this case, paramagnetic Ti^{3+} sites localized in the rutile part of the hybrid particle are not observed. When a material is irradiated with low-energy visible radiation ($\lambda > 420$ nm) obtained using an L42 filter (Hoya Corporation, Japan), an EPR signal also arises from Ti^{3+} sites in the anatase part of the particle, although such radiation is mainly absorbed in the rutile part with a bandgap of 3 eV. This indicates that in the case of irradiation of the material with visible

light, the photoelectrons generated in rutile diffuse into the anatase part of the particle and are captured there on bare Ti^{4+} ions forming Ti^{3+} centers.

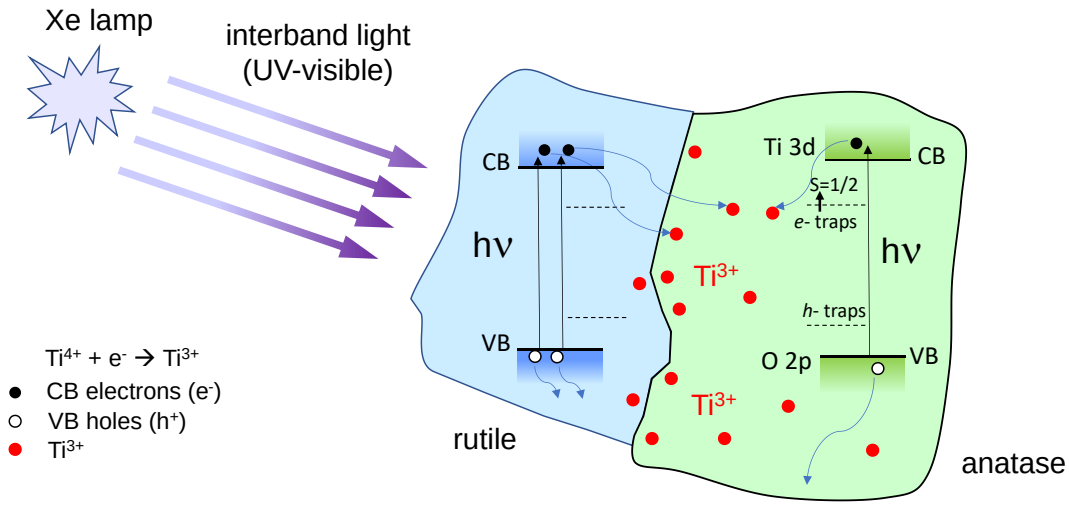

Figure S3. Scheme of interband optical transitions leading to the capture of photoelectrons in rutile- anatase compound particles. CB- conductive band (edge), VB- valence band (edge), Ti^{3+} - sites capturing photogenerated electrons according to the scheme $Ti^{4+} + e^- \rightarrow Ti^{3+}$, $h\nu$ - the energy of a quantum of light absorbed in a material.

References

S1. X. H. Wang, J.-G. Li, H. Kamiyama, M. Katada, N. Ohashi, Y. Moriyoshi and T. Ishigaki. *J. Am. Chem. Soc.*, 2005, **127**, 10982.

S2. C. Zhang, M. Ikeda, T. Uchikoshi, J.-G. Li, T. Watanabe and T. Ishigaki. *J. Mater. Res.*, 2011, **26**, 658.

S3. X. H. Wang, J.-G. Li, H. Kamiyama, Y. Moriyoshi and T. Ishigaki, *J. Phys. Chem. B*, 2006, **110**, 6804.

S4. Y. Nakada, *Master's thesis*, Hosei University, Japan, 2015. (Hosei University Repository, available on-line via URL: http://hdl.handle.net/10114/11731).